Average value of the DC-link output voltage in multi-phase uncontrolled bridge rectifiers under supply voltage balance and unbalance conditions

Jaume Saura [1], Juan Jose Mesas [2*], Luis Sainz [3]

[1] Department of Electrical Engineering, ESEIAAT-UPC, C. Colom 1, 08222 Terrassa, Spain (jaume.saura@upc.edu)
[2] Department of Electrical Engineering, EEBE-UPC, Av. Eduard Maristany 16, 08019 Barcelona, Spain
[3] Department of Electrical Engineering, ETSEIB-UPC, Av. Diagonal 647, 08028 Barcelona, Spain (luis.sainz@upc.edu)
[*] Corresponding Author (juan.jose.mesas@upc.edu)

Abstract: Average value of the DC-link output voltage is a variable of interest in multi-phase uncontrolled bridge rectifiers. The aim of this paper is to present a new, effort-saving procedure capable of providing an accurate value of this variable, a value which can be later corrected considering the usually omitted voltage drops. The proposed method, based on the Cauchy's formula (1841), allows the limitations of the existing methods to be overcome and can be used under supply voltage balance and unbalance conditions. Time-domain simulations and experimental tests were conducted to show the usefulness of the method and validate its accuracy. Under supply voltage balance conditions, the new method allows results as accurate as those provided by analytical expressions available in the literature or time-domain simulations performed by any software to be obtained. Moreover, under supply voltage unbalance conditions, this method outperforms analytical expressions available in the literature and at least equals time-domain simulations performed by any software in terms of accuracy of the obtained results. Therefore, under supply voltage balance and unbalance conditions, the proposed method makes the mathematical effort required to elaborate analytical expressions or the computational effort required to perform time-domain simulations unnecessary. In addition, the new method provides suitable estimates of values experimentally determined.

Keywords: Average value · Output voltage · Uncontrolled bridge rectifier · Balance conditions · Unbalance conditions · Cauchy

Nomenclature

AC	Alternating Current
ASD	Adjustable Speed Drive
ATRU	Autotransformer Rectifier Unit
CCM	Continuous Conduction Mode
DC	Direct Current
EMTDC	Electromagnetic Transients including DC
HVDC	High-Voltage Direct Current
MEA	More-Electric Aircraft
PSCAD	Power System Computer Aided Design
rms	root mean square
TM	Trademark
$\partial\Omega_v$	phasorial convex hull boundary
S_m	m-th side of $\partial\Omega_v$
v_{DC}	diode bridge output voltage
V_{DC}	average value of v_{DC}
v_i	i-th AC phase sinusoidal voltage
$\underline{V}_i$	i-th AC phase voltage phasor
v_{ij}	AC line sinusoidal voltage from v_i and v_j
v_o	DC-link output voltage
V_o	average value of v_o
w	length of the orthogonal projection of $\partial\Omega_v$
Ω_v	phasorial convex hull

1 Introduction

Multi-phase uncontrolled bridge rectifiers are widely used in a number of applications such as high voltage DC (HVDC) transmission, adjustable speed drives (ASDs) and renewable energy conversion systems [1]. Another recent application of this sort of rectifiers is multi-pulse autotransformer rectifier units (ATRUs) [1], [2], [3], [4], [5], [6], [7], [8], which are becoming the most reliable way for DC generation in More-Electric Aircrafts (MEAs) [2], [3], [4], [5], [6], [7].

Average value of the DC-link output voltage is one of the main variables of interest in multi-phase uncontrolled bridge rectifiers, regardless of whether they are working under supply voltage balance or unbalance conditions. Once the value of this variable is determined by the corresponding procedure, this value must be corrected by subtracting the usually omitted voltage drops, i.e., those due to AC inductances and diodes [9]. Therefore, the aim of this paper is to present a new, effort-saving procedure capable of providing an accurate value of this variable, a value which can be later corrected considering the usually omitted voltage drops.

Calculation of the average value of the DC-link output voltage in multi-phase uncontrolled bridge rectifiers is an issue of great importance as it follows from the literature. This average value allows the DC-link output voltage ripple in these rectifiers to be quantified by using the ripple factor, i.e., the ratio of rms value of alternating component of the DC-link output voltage (rms ripple [9]) to the average value of this voltage. The higher the ripple factor the lesser the purity of rectifier DC-link output voltage. Ripple factor can be expressed as a function of the rectifier variables [10], [11], to suggest possible ways to reduce this factor.

As an example of how to benefit from the average output voltage to avoid the effects of an output voltage ripple in the voltage control loop, a method for digital control of a high power factor AC/DC converter employing

the power balance control technique to achieve a fast response of the output voltage control is presented in [12].

A research area that considers the average value of the DC-link output voltage is open-circuit fault diagnosis in multi-phase uncontrolled bridge rectifiers. Most of the existing open-circuit fault diagnosis methods are based on harmonic analysis of the DC-link output voltage, which entails applying a numerical procedure (fast Fourier transform) [13], [14], [15], [16], or its analytical equivalent procedure [17], [18], to this voltage to obtain all the terms of the Fourier series, one of them being the average value of the DC-link output voltage. It must be noted that these fault diagnosis methods mostly rely on the harmonic terms of the Fourier series. However, a more accurate open-circuit fault diagnosis method for multi-phase uncontrolled bridge rectifiers mainly based on the average value of the DC-link output voltage is proposed in [19].

Suitable models of multi-pulse ATRUs are needed to study these ATRUs in a more efficient and effective way. To this end, functional models of P type symmetric and asymmetric 18-pulse ATRUs allowing accelerated and accurate simulations to be performed were developed in [3], [4], [5]. An important step in the development of these models is to express the average value of the DC-link output voltage as a function of the peak value of the AC phase voltage, which is usually achieved by analytical integration. The expressions deduced in [3], [4], [5], for P type symmetric and asymmetric 18-pulse ATRUs are similar to that provided in [8] for P type 12-pulse ATRUs. More general expressions than that deduced in [3], [5], for P type asymmetric 18-pulse ATRUs, and than that provided in [8] for P type 12-pulse ATRUs, are obtained in [2] by analytical integration but assuming several approximations.

Authors of references [20], [21] and [22] pioneered the elaboration of approximate analytical formulae for calculation of the average output voltage in one-/two-phase half-wave and full-wave diode rectifiers. More recently, other researchers have developed analytical formulae for calculation of the average output voltage in multi-pulse diode rectifiers [23]. Nowadays, the availability of several simulation tools such as PSCAD/EMTDC allows time-domain simulations to be performed and then numerical methods for calculation of the average output voltage to be applied.

As a result of the above literature review, it can be stated that there are different procedures to calculate the average value of the DC-link output voltage in multi-phase uncontrolled bridge rectifiers, which can be classified into numerical and analytical methods. The main numerical methods, which are mostly used under supply voltage unbalance conditions, are Fourier series and numerical integration of DC-link output voltage discrete values over a semi-period of the AC supply voltages. Not only do both numerical methods require previously obtaining and storing these DC-link output voltage discrete values, but also offer limited accuracy that depends on the discretization level. On the other hand, analytical methods, which are commonly employed under supply voltage balance conditions, provide closed-form analytical expressions of the average value of the DC-link output voltage mainly obtained from analytical integration of a piecewise continuous function over a semi-period of the AC supply voltages. These methods are a better option than numerical ones because they could provide exact analytical expressions as a function of the rectifier variables to further investigate their influence on rectifier behaviour. However, especially under supply voltage unbalance conditions, it is difficult to determine these expressions, which are usually obtained by assuming several approximations, resulting in a loss of accuracy.

In all the modern applications, the DC-link output voltage provided by multi-phase uncontrolled bridge rectifiers is feeding some kinds of power electronic devices. These devices must be fed within a safe operating voltage range, which means that they effectively reject the DC-link output voltage if its average value is out of this range. Therefore, underestimation of this average value by using the existing methods (for example, the analytical expressions numbered as (17) and (18) in [2]) becomes a problem only if the actual average value is above any of the range bounds, with the estimated average value below this bound. Likewise, overestimation of this average value by using the existing methods becomes a problem only if the actual average value is below any of the range bounds, with the estimated average value above this bound. Both problems lead to unexpected acceptances or unexpected rejections by power electronic devices of the DC-link output voltage provided by multi-phase uncontrolled bridge rectifiers.

With the purpose of overcoming the above limitations of the existing methods, thus avoiding the problems derived from such limitations, this paper presents a new method to calculate the average value of the DC-link output voltage in multi-phase uncontrolled bridge rectifiers from the AC supply voltages. This method, based on the Cauchy's formula (1841) [24], [25], can be used under supply voltage balance and unbalance conditions by only assuming the usual hypotheses of continuous current conduction mode (CCM) operation and negligible voltage drops due to AC inductances and diodes. The method strengths over other existing ones are:

- Unlike with numerical methods, there is no need for obtaining and storing the DC-link output voltage discrete values over a semi-period of the AC supply voltages and then treating these DC-link output voltage discrete values with any simulation software. This implies considerable saving in computational effort.
- In contrast to analytical methods, it is unnecessary to analytically integrate a piecewise continuous function over a semi-period of the AC supply voltages. This results in considerable saving in mathematical effort, especially under supply voltage unbalance conditions.
- Compared to existing ones, the new method always provides exact values, since it is not subject to discretizations or approximations.

The conducted methodology at presenting and analysing the new method is clearly reflected in the organization of the paper as follows. Section 2 shows the multi-phase uncontrolled bridge rectifier circuit and establishes the link between the diode bridge output voltage and the length of the orthogonal projection of a phasorial convex hull boundary onto an axis. In Section 3, a description of existing methods to calculate the average value of the DC-link output voltage in multi-phase uncontrolled bridge rectifiers is given. In Section 4, the link

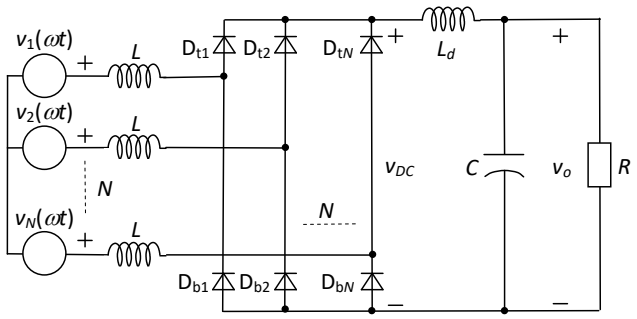

Fig. 1 Multi-phase uncontrolled bridge rectifier circuit

established in Section 2 is used to obtain the new method for calculating the above average value, the applicability of which is illustrated and detailed. Section 5 presents two applications in multi-pulse ATRUs to show the usefulness of the proposed method and validate its accuracy. In Section 6, the most important results obtained in Section 5 are discussed. Finally, Section 7 draws conclusions from these results.

2 Multi-phase uncontrolled bridge rectifiers

Fig. 1 shows a multi-phase uncontrolled bridge rectifier with the AC inductance L, the output LC filter inductance L_d and capacitance C, and the load represented as a resistor of resistance R. The rectifier is fed by AC phase unbalanced sinusoidal voltages,

$$v_i(\omega t) = V_i \cos(\omega t + \alpha_i) \qquad (i = 1 \ldots N), \qquad (1)$$

where N is the number of the phases ($N \geq 2$), $\omega = 2\pi/T = 2\pi f$ is the angular frequency of the sinusoidal supply voltages and T and $f = 1/T$ are the period and the frequency of the supply voltages, respectively.

In nominal circuit operation, the output LC filter inductance L_d keeps the rectifier operating in CCM and the output LC filter capacitance C is large enough to keep the DC-link output voltage $v_o(\omega t)$ close to a constant value. The average value of $v_o(\omega t)$, called V_o, is one of the main variables to analyse the behaviour of uncontrolled bridge rectifiers. The voltage V_o matches with the average value of the diode bridge output voltage $v_{DC}(\omega t)$, called V_{DC}, (i.e., $V_o = V_{DC}$,) because the DC component of the voltage drop in the inductor L_d is zero. Moreover, assuming CCM operation, negligible voltage drops due to AC inductances (AC line inductance, and supply transformer leakage inductance), and negligible diode voltage drops, $v_{DC}(\omega t)$ is directly related to the AC line voltages $v_{ij}(\omega t) = v_i(\omega t) - v_j(\omega t)$. As an example, Fig. 2(a) shows the AC phase sinusoidal voltages $v_i(\omega t)$ with $f = 50$ Hz and the voltage $v_{DC}(\omega t)$ of a 6-phase uncontrolled bridge rectifier under supply voltage unbalance conditions. It can be observed that both the diode of the rectifier top diodes (D_{t1} to D_{tN} in Fig. 1) with its cathode at the highest AC phase voltage and the diode of the rectifier bottom diodes (D_{b1} to D_{bN} in Fig. 1) with its anode at the lowest AC phase voltage conduct. Thus, the voltage $v_{DC}(\omega t)$ is equal to the difference between the maximum and minimum values of the AC phase voltages, i.e. the AC line voltages, at each conduction time of the top and bottom diodes (see Fig. 2(a)), i.e.,

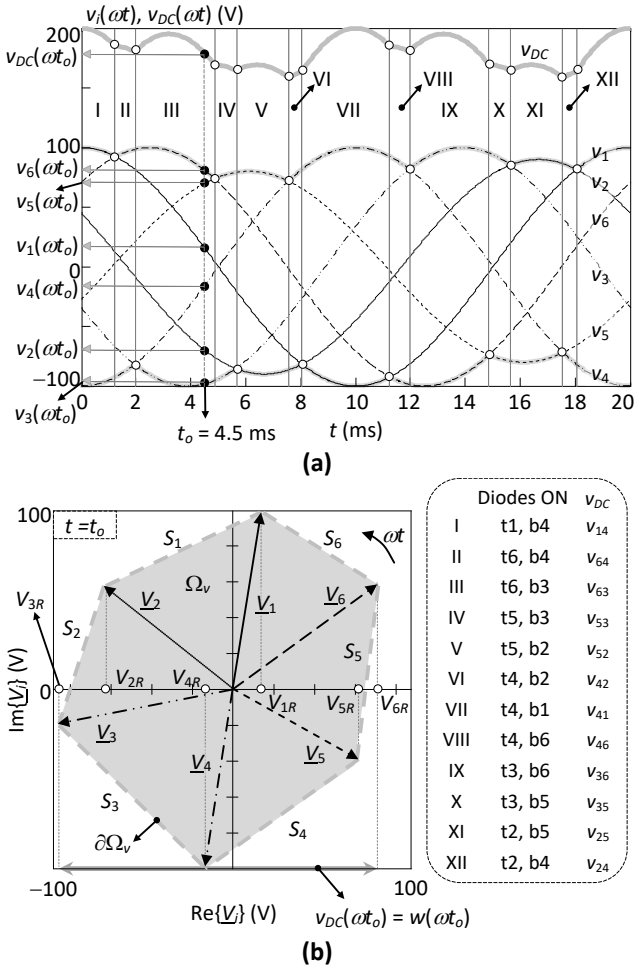

Fig. 2 Study of a 6-phase uncontrolled bridge rectifier
(a) AC phase voltages and diode bridge output voltage, **(b)** Phasor diagram of the AC phase voltages at t_o = 4.5 ms

$$v_{DC}(\omega t) = \max_{1 \leq i \leq N} \{v_i(\omega t)\} - \min_{1 \leq i \leq N} \{v_i(\omega t)\}. \qquad (2)$$

The AC phase sinusoidal voltages can be represented with phasors in the Gauss complex plane as

$$v_i(\omega t) = V_i \cos(\omega t + \alpha_i) = \mathrm{Re}\left\{\underline{V}_i e^{j\omega t}\right\} \quad (i = 1 \ldots N), \quad (3)$$

where $\underline{V}_i = V_i e^{j\alpha i}$ are the AC phase voltage phasors. Therefore, it can be deduced from (2) and (3) that

$$v_{DC}(\omega t) = \max_{1 \leq i \leq N} \left\{\mathrm{Re}\left\{\underline{V}_i e^{j\omega t}\right\}\right\} - \min_{1 \leq i \leq N} \left\{\mathrm{Re}\left\{\underline{V}_i e^{j\omega t}\right\}\right\}. \quad (4)$$

Fig. 2(b) shows the phasor diagram representation of the AC phase voltages in Fig. 2(a) (i.e., $\underline{V}_i$ with i = 1 to 6) at the time instant t_o = 4.5 ms. It can be observed that the real parts of the phasors (i.e., the orthogonal projections V_{iR} of the phasors onto the horizontal axis) in Fig. 2(b) are the values of the AC phase voltages in Fig. 2(a) at the instant of the phasor representation, i.e., $\mathrm{Re}\{\underline{V}_i\} = V_{iR}$ in Fig. 2(b) are equal to $v_i(\omega t_o)$ in Fig. 2(a). According to (4), $v_{DC}(\omega t)$ at each time instant is equal to the difference between the highest and lowest real parts of the AC phase voltage phasors at that time instant (e.g., $v_{DC}(\omega t_o) = \mathrm{Re}\{\underline{V}_6\} - \mathrm{Re}\{\underline{V}_3\} = V_{6R} - V_{3R}$).

Fig. 2(b) also depicts the convex hull Ω_v of the set of ends of the AC phase voltage phasors (phasorial convex hull) at the time instant t_o = 4.5 ms, which is defined as the smallest convex region enclosing all ends in the set. It can be noted that the difference between the highest and lowest real parts of the AC phase voltage phasors in Fig. 2(b) equates to the length w of the orthogonal projection of the phasorial convex hull boundary $\partial\Omega_v$ onto the horizontal axis at the instant of the phasor representation, i.e., both $\mathrm{Re}\{\underline{V}_6\} - \mathrm{Re}\{\underline{V}_3\} = V_{6R} - V_{3R}$ and $w(\omega t_o)$ are equal in Fig. 2(b). This can be generalized to any time instant, leading to

$$\max_{1\le i\le N}\left\{\mathrm{Re}\left\{\underline{V}_i e^{j\omega t}\right\}\right\} - \min_{1\le i\le N}\left\{\mathrm{Re}\left\{\underline{V}_i e^{j\omega t}\right\}\right\} = w(\omega t). \quad (5)$$

Consequently, it can be deduced from (4) and (5) that

$$v_{DC}(\omega t) = w(\omega t). \quad (6)$$

3 Average value of the DC-link output voltage in multi-phase uncontrolled bridge rectifiers

The average value of the DC-link output voltage, V_o, characterizes the behaviour of the multi-phase uncontrolled bridge rectifiers. This value can also be determined from the average value of the diode bridge output voltage, V_{DC}. There are different methods to calculate the voltage V_{DC}:

- Numerical methods:

  These methods use discrete values of $v_{DC}(\omega t)$ during a semi-period $T/2$ of the AC phase voltages in order to numerically obtain the value of V_{DC}. The main approaches are:

  - Fourier series. The voltage V_{DC} is obtained from the first term of the Fourier series of $v_{DC}(\omega t)$ which can be easily determined by applying the MATLAB function *fft*(·) to $v_{DC}(\omega t)$ over a semi-period,

  $$v_{DC}(\omega t) = V_{DC} + \sum_{k=1}^{\infty} V_{DCk}\cos(k\omega t + \beta_k). \quad (7)$$

  - Numerical integration. The voltage V_{DC} can be numerically obtained dividing the numerical integration of $v_{DC}(\omega t)$ over a semi-period by the semi-period length,

  $$V_{DC} = \frac{1}{T/2}\sum_{t=0}^{T/2-\Delta t}\frac{v_{DC}(\omega(t+\Delta t)) + v_{DC}(\omega t)}{2}\cdot\Delta t. \quad (8)$$

  This value can also be obtained by applying the MATLAB function *mean*(·) to $v_{DC}(\omega t)$ over a semi-period.

- Analytical methods:

  These methods are useful to have closed-form analytical expressions for determining V_{DC} as a function of the rectifier variables to further investigate their influence. In general, CCM operation and negligible voltage drops due to AC inductances and diodes are assumed, which allows the expression for V_{DC} calculation to be obtained from the AC phase voltages.

  - Analytical formulae. There exists a well-known expression for calculation of V_{DC} in multi-phase uncontrolled bridge rectifiers which are fed by AC phase balanced sinusoidal voltages [26],

  $$V_{DC} = 2\frac{NV}{\pi}\sin\left(\frac{\pi}{N}\right), \quad (9)$$

  where V is the peak value of the AC phase balanced sinusoidal voltages and N is the number of phases of the rectifier. In addition, there are a few expressions for calculation of V_{DC} under supply voltage unbalance conditions derived from studies on multi-pulse ATRUs [2]. Nevertheless, these expressions are only valid for specific supply voltage unbalance conditions and they are obtained by assuming several approximations.

  - Analytical integration. An expression for calculation of V_{DC} can also be obtained dividing the analytical integration of $v_{DC}(\omega t)$ over a semi-period by the semi-period length. Taking into account that $v_{DC}(\omega t)$ is a piecewise continuous function on the interval [0, $T/2$], this integration is made from the corresponding AC line voltage expressions by splitting the interval into subintervals $[t_k, t_{k+1}]$ at N_{bp} breakpoints,

  $$V_{DC} = \frac{1}{T/2}\int_{t=0}^{T/2} v_{DC}(\omega t)dt = \frac{1}{T/2}\sum_{k=0}^{N_{bp}}\left(\int_{t=t_k}^{t_{k+1}} v_{ij}(\omega t)dt\right), \quad (10)$$

  where the time instants t_k of the breakpoints must be previously determined as

  $$t_k = \begin{cases} 0 & k = 0 \\ \frac{1}{\omega}\tan^{-1}\left(\frac{V_i\cos(\alpha_i) - V_j\cos(\alpha_j)}{V_i\sin(\alpha_i) - V_j\sin(\alpha_j)}\right) & 1 \le k \le N_{bp} \\ T/2 & k = N_{bp}+1 \end{cases}. \quad (11)$$

  Under supply voltage balance conditions, (9) is obtained from (10). Under supply voltage unbalance conditions, this approach would allow closed-form analytical expressions for calculation of V_{DC} to be obtained without carrying out any approximation, but involving a great mathematical effort.

On one hand, it must be noted that numerical methods allow V_{DC} to be numerically calculated, but the accuracy of the obtained value depends on the discretization of $v_{DC}(\omega t)$. On the other hand, analytical methods allow closed-form expressions for calculation of V_{DC} to be obtained:

- Under supply voltage balance conditions, an exact expression (disregarding AC inductance and diode voltage drops) for any number of phases of the rectifier is obtained in (9).
- Under supply voltage unbalance conditions, exact expressions (disregarding AC inductance and diode voltage drops) could be obtained with a great mathematical effort. This effort increases with the number of phases of the rectifier.

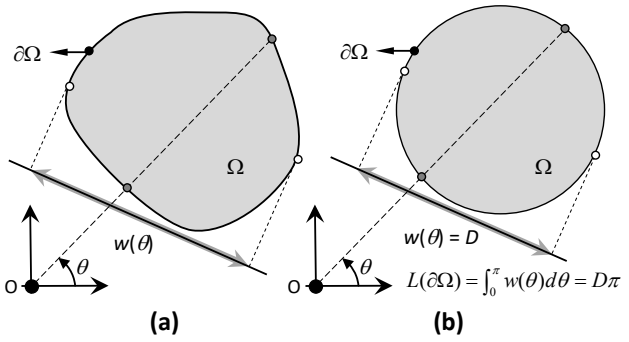

Fig. 3 Cauchy's formula (1841)
(a) General bounded convex domain, **(b)** Circular bounded convex domain

4 New method for calculation of the average value of the DC-link output voltage

To overcome the drawbacks of the previous methods, a new approach, called phasorial convex hull method, is proposed to calculate the average value of the DC-link output voltage V_o from V_{DC}. This method can be used with multi-phase uncontrolled bridge rectifiers under supply voltage balance and unbalance conditions by only assuming the usual hypotheses of CCM operation and negligible voltage drops due to AC inductances and diodes.

4.1 Phasorial convex hull method

The new approach allows the average value of $v_{DC}(\omega t)$ in multi-phase uncontrolled bridge rectifiers under supply voltage balance and unbalance conditions to be obtained by applying the following simple expression,

$$V_{DC} = \frac{L(\partial\Omega_v)}{\pi}, \tag{12}$$

where $L(\partial\Omega_v)$ is the length of the phasorial convex hull boundary $\partial\Omega_v$ (see Fig. 2(b)),

$$\partial\Omega_v = \bigcup_{m=1}^{6} S_m \;\Rightarrow\; L(\partial\Omega_v) = \sum_{m=1}^{6} L(S_m), \tag{13}$$

with S_m being the m-th side of $\partial\Omega_v$ in (13).

Proof: Let Ω be a bounded convex domain, let θ be the rotation angle of Ω with respect to the origin of the Gauss complex plane, and let $w(\theta)$ be the length of the orthogonal projection of the convex domain boundary $\partial\Omega$ onto a given straight line (see Fig. 3(a)). Then Cauchy's formula (1841) [24], [25], asserts that the length of $\partial\Omega$, $L(\partial\Omega)$, can be determined as follows

$$L(\partial\Omega) = \int_0^{\pi} w(\theta)d\theta. \tag{14}$$

Considering (6), $v_{DC}(\omega t)$ at each time instant is equal to $w(\omega t)$ (see the example in Fig. 2(b)). Therefore,

$$\frac{1}{T/2}\int_0^{T/2} v_{DC}(\omega t)dt = \frac{1}{\pi}\int_0^{\pi} w(\omega t)d(\omega t). \tag{15}$$

Consequently, it can be deduced from (14) and (15)

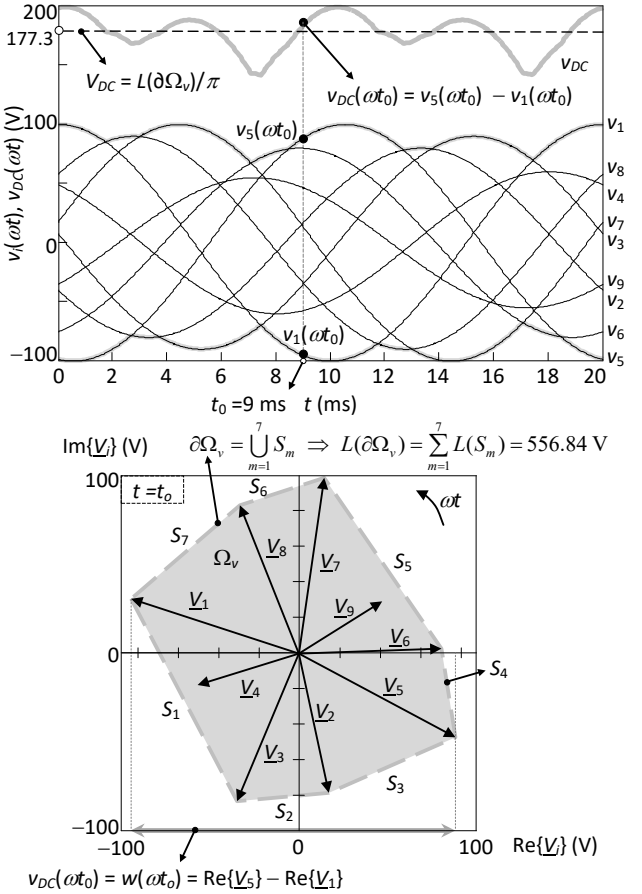

Fig. 4 Phasorial convex hull method

that

$$V_{DC} = \frac{L(\partial\Omega)}{\pi}. \tag{16}$$

Examples: Three examples are presented to illustrate the application of the Cauchy's formula (1841) and the phasorial convex hull method.

- Example #1: The Cauchy's formula (1841) is applied in Fig. 3(b) to calculate the length of a circumference.
- Example #2: (9) is derived from (12), since the magnitude of the corresponding AC line voltage phasors of an N-phase uncontrolled bridge rectifier under supply voltage balance conditions, $2\cdot V\cdot\sin(\pi/N)$, is multiplied by the number of phases N to obtain the length of $\partial\Omega_v$, and then divided by π.
- Example #3: Fig. 4 shows the AC phase sinusoidal voltages and the voltage phasor diagram of a 9-phase uncontrolled bridge rectifier under supply voltage unbalance conditions. It is noted from Fig. 4 that the proposed approach can be applied even when the AC phase voltages of some phases do not work (e.g., AC phase voltages of both 4th and 9th phases) or the AC phase voltage phasors of consecutive phases are not consecutive in the Gauss complex plane (e.g., AC phase voltage phasors of 1st and 2nd phases). Moreover, the approach could also be applied when the origin of the Gauss complex plane does not

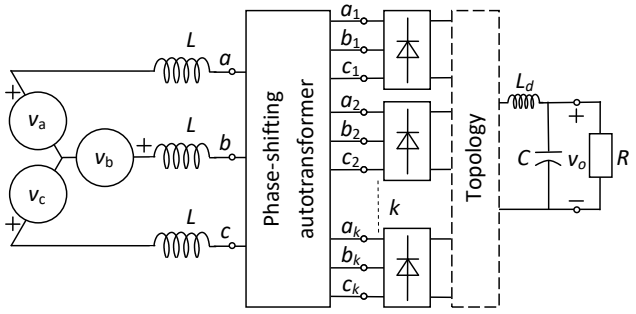

Fig. 5 Multi-pulse ATRU

belong to the phasorial convex hull Ω_v or the phasorial convex hull degenerates in a segment.

4.2 Procedure to apply the phasorial convex hull method

The procedure to apply the phasorial convex hull method consists of four steps:

1) Draw in a Gauss complex plane the AC phase voltage phasors $\underline{V}_i$ (i = 1 to N) which feed the multi-phase uncontrolled bridge rectifier.
2) Determine the convex hull Ω_v of the set of ends of the AC phase voltage phasors (phasorial convex hull). This can be carried out by applying the MATLAB function *convhull*(·) to the set of ends of the AC phase voltage phasors.
3) Calculate the length of the phasorial convex hull boundary $\partial\Omega_v$,

$$L(\partial\Omega_v) = \sum_{m=1}^{N_S} L(S_m) = \sum_{m=1}^{N_S} \left\| \underline{V}_i^m - \underline{V}_j^m \right\|, \qquad (17)$$

where N_S is the number of sides of the phasorial convex hull boundary $\partial\Omega_v$, and $\underline{V}^m{}_i$, $\underline{V}^m{}_j$ are the AC phase voltage phasors characterizing the side S_m.

4) Use (12) to determine V_{DC}.

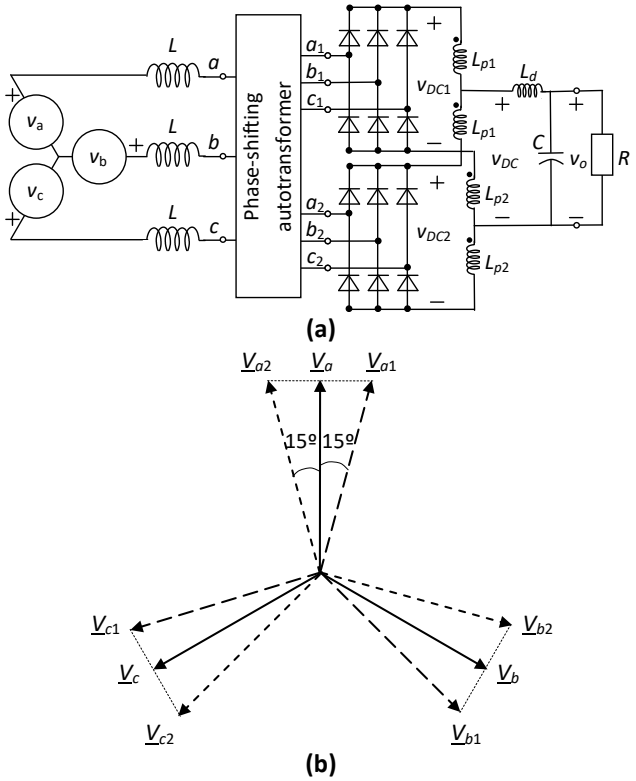

Fig. 6 P type 12-pulse ATRU with interphase reactors
(a) ATRU configuration, **(b)** Voltage phasor diagram

5 Applications

Two applications in multi-pulse ATRUs (i.e., PSCAD/EMTDC time-domain simulations and experimental tests) are presented to show the usefulness of the phasorial voltage convex hull method as well as to validate the accuracy of the proposed approach.

Multi-pulse ATRUs are becoming the basis for future DC generation of several electric applications such as aircraft electric systems [2], [3], [4], [5], [6], [7], and wind energy conversion systems [8]. According to Fig. 5, they are formed by multiple three-phase uncontrolled bridge rectifiers connected to each other in two main topologies, parallel (P type) and series (S type), and fed by a phase-shifting autotransformer supplied by three input voltages

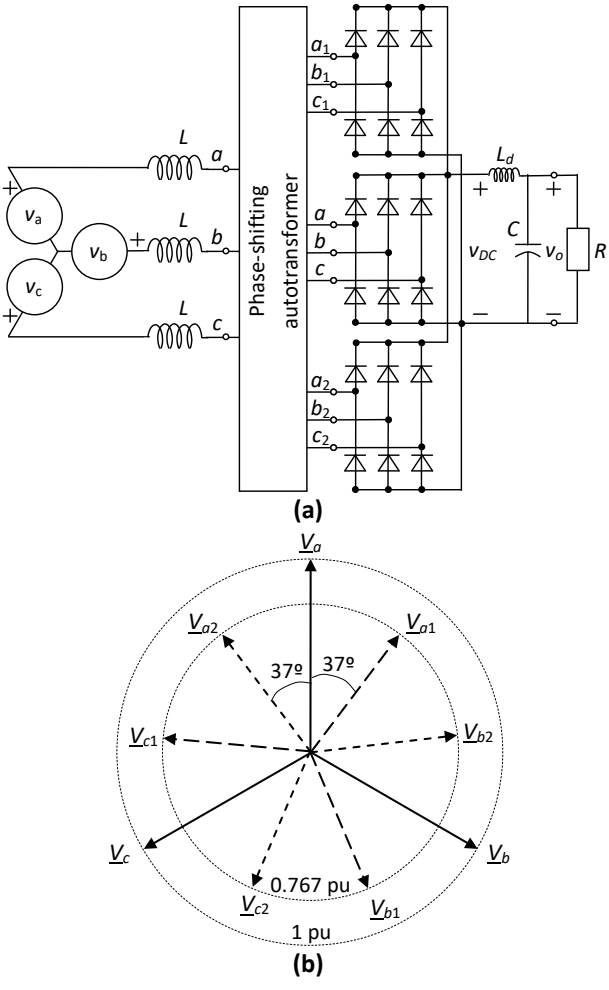

Fig. 7 P type asymmetric 18-pulse ATRU without interphase reactors
(a) ATRU configuration, **(b)** Voltage phasor diagram

$$
\begin{aligned}
v_a(\omega t) &= \sqrt{2}V_a \cos(\omega t + \alpha_a) \\
v_b(\omega t) &= \sqrt{2}V_b \cos(\omega t + \alpha_b) \\
v_c(\omega t) &= \sqrt{2}V_c \cos(\omega t + \alpha_c) \qquad (\omega = 2\pi f),
\end{aligned} \tag{18}
$$

where V_a, V_b and V_c and α_a, α_b and α_c are the rms values and the phase angles of the input voltages, respectively. The P type 12- and 18-pulse ATRU configurations are the most commonly used [2], [8], [27], and [2], [3], [4], [5], [6], [7], respectively.

The average value of the DC-link output voltage V_o in multi-pulse ATRUs is usually determined by applying the numerical methods in Section 3 to time-domain simulations due to the difficulty for obtaining analytical expressions for all multi-pulse ATRU configurations and supply voltage conditions. On one hand, some studies provide analytical expressions to calculate V_o under supply voltage balance conditions (i.e., $V_a = V_b = V_c = V_s$, $\alpha_b = \alpha_a - 2\pi/3$ and $\alpha_c = \alpha_a + 2\pi/3$) for specific multi-pulse ATRUs [3], [4], [5], [8]. On the other hand, only a few studies present analytical expressions to calculate V_o under supply voltage unbalance conditions, and these expressions are always for particular multi-pulse ATRUs and specific supply voltage unbalance conditions [2]. The phasorial convex hull method could be an easy and powerful tool to calculate V_o under any supply voltage unbalance conditions.

5.1 PSCAD/EMTDC time-domain simulations

As an example, the calculation of V_o in a P type 12-pulse ATRU with interphase reactors, Fig. 6(a), and a P type asymmetric 18-pulse ATRU without interphase reactors, Fig. 7(a), fed by the AC phase voltage phasors in the diagrams of Fig. 6(b) and Fig. 7(b) is illustrated. Considering CCM operation, negligible voltage drops due to AC inductances (AC line inductance, supply transformer leakage inductance, and phase-shifting autotransformer leakage inductance), and negligible diode voltage drops, both ATRUs are studied in [2] where analytical expressions to calculate V_o under specific supply voltage unbalance conditions ($V_a = \lambda_a V_c$, $V_b = \lambda_b V_c$ and $V_c = V_s$, with $\lambda_a \geq \lambda_b \geq 1$ and $\alpha_b = \alpha_a - 2\pi/3$ and $\alpha_c = \alpha_a + 2\pi/3$) are obtained by assuming several approximations,

$$
\begin{aligned}
V_o^{(12-\mathrm{p})} &\approx 2.42\left(\frac{\lambda_a + \lambda_b + 1}{3}\right)V_s \\
V_o^{(18-\mathrm{p})} &\approx 2.437\left(\frac{\lambda_a + \lambda_b + 1}{3}\right)V_s.
\end{aligned} \tag{19}
$$

The phasorial convex hull method allows V_o to be accurately calculated under any supply voltage unbalance conditions. In particular, it allows more accurate results of V_o than those of the above study to be obtained:

- The P type 12-pulse ATRU in Fig. 6(a) results from connecting two three-phase uncontrolled bridge rectifiers in parallel by means of the interphase reactors L_{p1} and L_{p2} at the output terminals of each rectifier [2], [8], [27]. These reactors absorb the voltage difference between DC voltages of the three-phase uncontrolled bridge rectifiers at any instant and ensure their independent operation without any circulating current. According to this, the diode bridge output voltage, v_{DC}, can be expressed from the diode bridge output voltages of each rectifier, v_{DC1} and v_{DC2}, as [8]

$$
v_{DC} = \frac{1}{2}(v_{DC1} + v_{DC2}), \tag{20}
$$

and the average values of the diode bridge and the DC-link output voltages, V_{DC} and V_o, are

$$
V_o = V_{DC} = \frac{1}{2}(V_{DC1} + V_{DC2}). \tag{21}
$$

Considering the AC phase voltage phasors in the diagram of Fig. 6(b), it can be asserted that $V_{DC1} = V_{DC2}$, and therefore $V_{DC} = V_{DC1} = V_{DC2}$ (21). Thus, the average value of the DC-link output voltage V_o can be calculated from V_{DC1} or V_{DC2} by applying the procedure in Section 4.2 to the AC phase voltage phasors $\underline{V}_{a1}$, $\underline{V}_{b1}$ and $\underline{V}_{c1}$, or $\underline{V}_{a2}$, $\underline{V}_{b2}$ and $\underline{V}_{c2}$, in the diagram of Fig. 6(b). An analytical expression is provided in [8] for calculation of V_o under supply voltage balance conditions. According to the previous comments, this expression can also be obtained by applying (9) with $N = 3$ and considering the AC phase voltage phasors in the diagram of Fig.

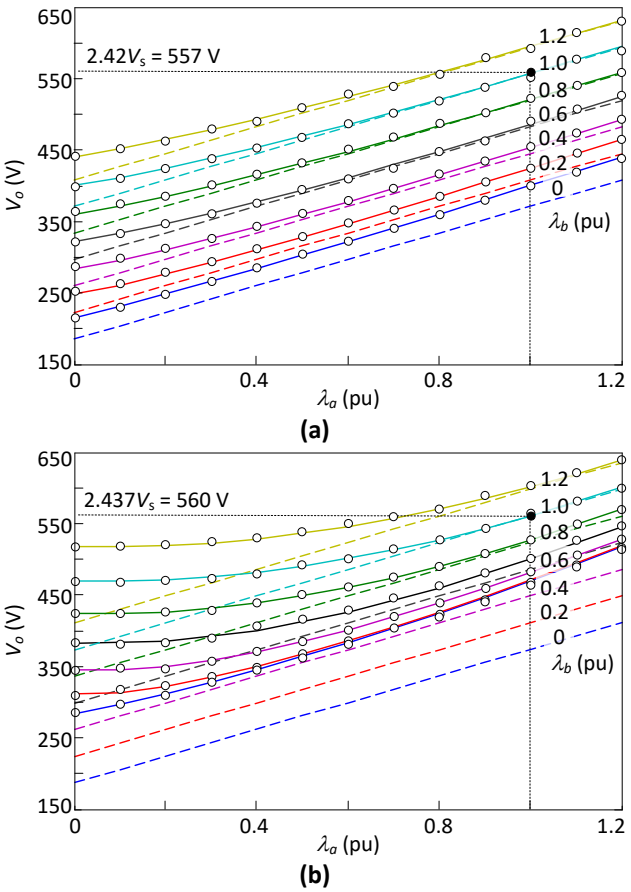

Fig. 8 Average value of the DC-link output voltage V_o of ATRUs with V_s = 230 V [(12) in continuous lines, (19) in dashed lines and PSCAD/EMTDC time-domain simulations in dots]
(a) P type 12-pulse ATRU, **(b)** P type asymmetric 18-pulse ATRU

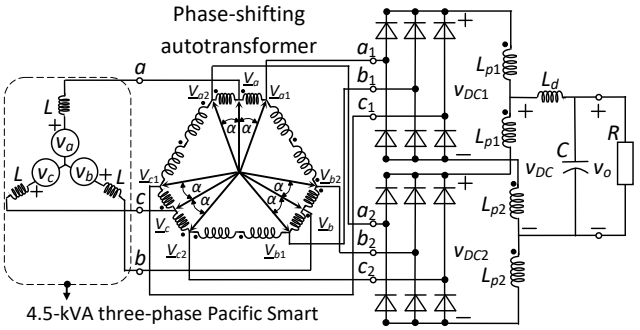

Fig. 9 Experimental setup
(a) Diagram, **(b)** Photograph

6(b),

$$V_o = V_{DC1} = 2\frac{3\sqrt{2}\,V_s/\cos(15^o)}{\pi}\sin\left(\frac{\pi}{3}\right) = 2.42V_s. \quad (22)$$

- The P type asymmetric 18-pulse ATRU in Fig. 7(a) is formed by three three-phase uncontrolled bridge rectifiers with their output terminals directly connected in parallel [2], [3], [4], [5], [6], [7], resulting the nine−phase uncontrolled bridge rectifier in Fig. 1 with $N = 9$. This rectifier is supplied with the asymmetrical AC phase voltage phasors in Fig. 7(b). Thus, the average value of the DC-link output voltage V_o can be calculated by applying the procedure in Section 4.2 to the AC phase voltage phasors in Fig. 7(b). An analytical expression is deduced in [3], [5], for calculation of V_o under supply voltage balance conditions,

$$V_o = \sqrt{6}V_s\frac{\sin(\pi/18)}{\pi/18} = 2.437V_s. \quad (23)$$

This expression cannot be obtained by applying (9) with $N = 9$ because the AC phase voltage phasors at the terminals of the nine-phase uncontrolled bridge rectifier are unbalanced (see diagram of Fig. 7(b)).

Considering $V_s = 230$ V, Fig. 8 compares the average values of the DC-link output voltage V_o obtained from both the phasorial convex hull method and (19) for different values of λ_a and λ_b, as well as the value of V_o obtained from (22) and (23) under supply voltage balance conditions.

Table 1 ATRU data

α (º)	$L_{p1} = L_{p2}$ (mH)	L_d (mH)	C (μF)	R (Ω)
19	1.68 ($R_{int} \approx 0.108\ \Omega$)	10 ($R_{int} \approx 0.4\ \Omega$)	96	42

Moreover, the accuracy of the phasorial convex hull method and (19) is checked in Fig. 8 from PSCAD/EMTDC time-domain simulations. It is observed that the phasorial convex hull method always provides accurate results whereas the expressions in (19) are only valid for low unbalance degrees.

5.2 Experimental tests

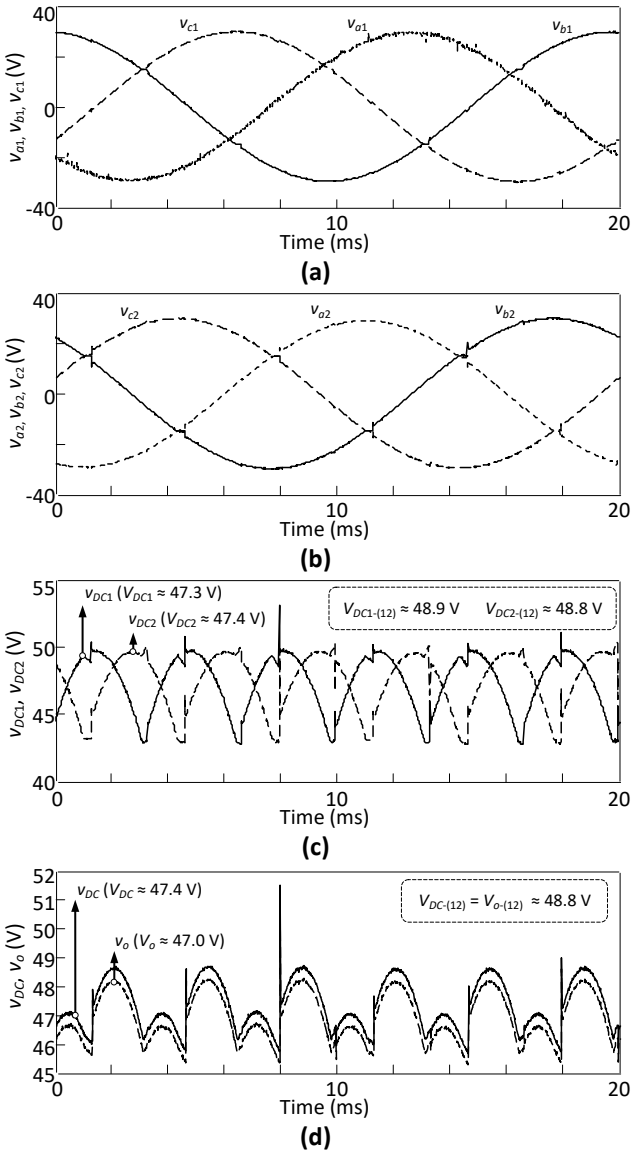

Fig. 10 Test A
(a) Input voltages of rectifier 1, **(b)** Input voltages of rectifier 2, **(c)** Diode bridge output voltages of rectifiers 1 and 2, **(d)** Diode bridge and DC-link output voltages of the ATRU

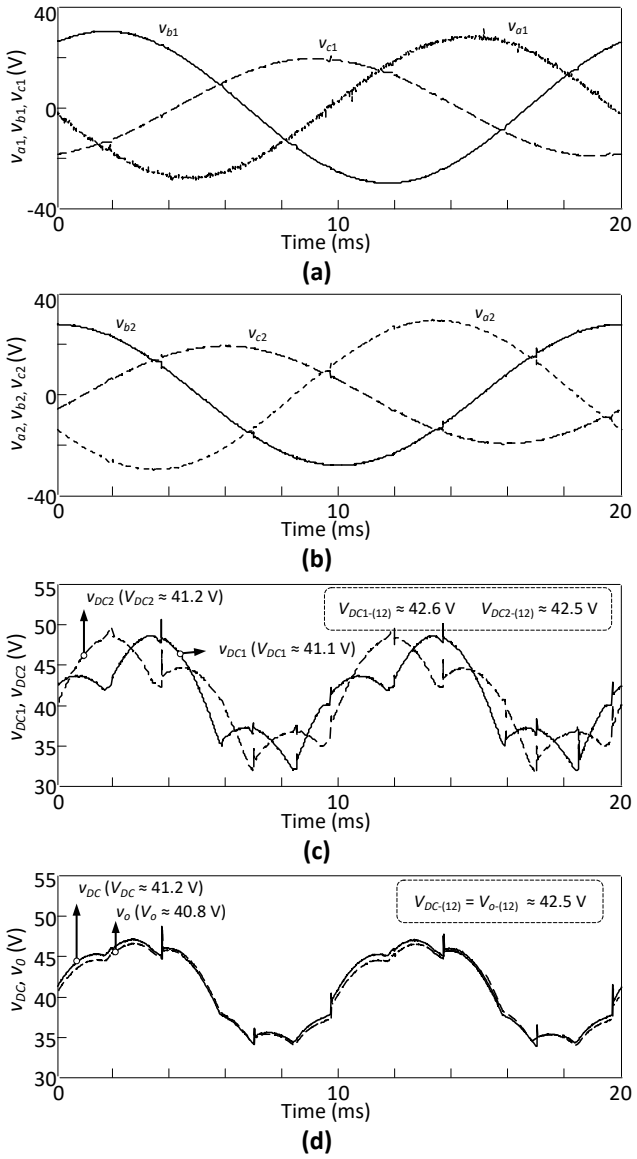

Fig. 11 Test B
(a) Input voltages of rectifier 1, **(b)** Input voltages of rectifier 2, **(c)** Diode bridge output voltages of rectifiers 1 and 2, **(d)** Diode bridge and DC-link output voltages of the ATRU

In order to experimentally validate the phasorial convex hull method, two experimental tests were conducted on the P type 12-pulse ATRU in Fig. 9 under different supply voltage conditions. It must be noted that CCM operation, negligible voltage drops due to AC inductances (AC line inductance, supply transformer leakage inductance and phase-shifting autotransformer leakage inductance), and negligible diode voltage drops, were checked in the experimental setup before performing the tests. ATRU data are presented in Table 1. The complete experimental setup is represented in Fig. 9(a) and photographed in Fig. 9(b). It consists of the following elements:

- (A) A 4.5 kVA three-phase Pacific Smart Source TM (345-AMX model) to feed the ATRU.
- (B) An oscilloscope Yokogawa TM DL850 to make recordings.
- (C) A laptop Acer TM to numerically process and then compare the recordings with the phasorial convex hull method results.
- (D) A phase-shifting autotransformer of phase-shifting angle α.
- (E) Two three-phase uncontrolled bridge rectifiers made up of Semikron TM SKKD 46/16 SEMIPACK 1 rectifier diode modules.
- (F) Interphase reactors of inductances L_{p1} and L_{p2} and internal resistances R_{int}.
- (G) An output LC filter inductor of inductance L_d and internal resistance R_{int}.
- (H) An output LC filter capacitor of capacitance C.
- (I) A load resistor of resistance R.

This experimental setup allowed the following tests to be carried out:

- Test A: The ATRU was fed with 20 V/50 Hz sinusoidal balanced three-phase voltages.
- Test B: The ATRU was fed with 50 Hz sinusoidal unbalanced three-phase voltages ($V_a = 20$ V, $V_b = 20$ V and $V_c = 12$ V, $\alpha_b = \alpha_a - 2\pi/3$ and $\alpha_c = \alpha_a + 2\pi/3$).

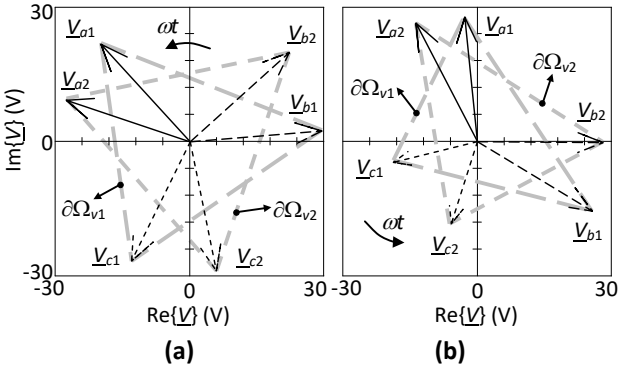

Fig. 12 Phasor diagrams at the time instant 0 ms
(a) Test A, **(b)** Test B

Fig. 10 and Fig. 11 show the different ATRU measured voltages. Moreover, the average values of the diode bridge and the DC-link output voltages measured in the experimental tests, V_{DC} and V_o, and calculated by the phasorial convex hull method (12), $V_{DC\text{-}(12)}$ and $V_{o\text{-}(12)}$, are labelled for comparison purposes. According to the phasor diagrams in Fig. 12, the phasorial convex hull method allows the average value of the diode bridge output voltage of either of the two three-phase rectifiers, $V_{DC1\text{-}(12)}$ or $V_{DC2\text{-}(12)}$, to be determined by applying (12) to the corresponding phasorial convex hull boundary, $\partial\Omega_{v1}$ or $\partial\Omega_{v2}$. Subsequently, the average values of the diode bridge and the DC-link output voltages, $V_{DC\text{-}(12)}$ and $V_{o\text{-}(12)}$, are determined by (21). Note that in scenarios of CCM operation and negligible voltage drops due to AC inductances and diodes, the proposed method is a practical and accurate approach for estimating the average value of the DC-link output voltage. The difference between the measured and calculated average voltages is mainly due to the internal resistances R_{int} of both the interphase reactors, L_{p1} and L_{p2}, and the output LC filter inductor, L_d (see Table 1). These internal resistances are not considered by the phasorial convex hull method.

6 Discussion of results

The accuracy of the phasorial convex hull method and the analytical expressions in (19) (obtained in [2]), in

(22) (provided in [8]) and in (23) (deduced in [3], [5]), was checked by PSCAD/EMTDC time-domain simulations in Subsection 5.1. The phasorial convex hull method and all the analytical expressions led to the same accurate results under supply voltage balance conditions. However, under supply voltage unbalance conditions, the analytical expressions in (22) and (23) were found to be inapplicable as expected because these expressions are only valid under supply voltage balance conditions. As for the analytical expressions in (19), whose accuracy was checked under the specific supply voltage unbalance conditions described in [2], it was shown that they are only valid for low unbalance degrees. Only the phasorial convex hull method provided results at least as accurate as those of PSCAD/EMTDC time-domain simulations regardless of the supply voltage unbalance degree. Therefore, under supply voltage balance and unbalance conditions, the new method makes the mathematical effort required to elaborate analytical expressions or the computational effort required to perform PSCAD/EMTDC time-domain simulations unnecessary.

The accuracy of the phasorial convex hull method was also checked by two experimental tests in Subsection 5.2. Both under supply voltage balance (Test A) and unbalance (Test B) conditions, this new method provided results accurate enough to be used as suitable estimates of values experimentally determined, making it unnecessary to elaborate analytical expressions or perform PSCAD/EMTDC time-domain simulations for this purpose.

7 Conclusion

The paper presents the phasorial convex hull method for calculation of the average value of the DC-link output voltage in multi-phase uncontrolled bridge rectifiers from the AC supply balanced and unbalanced voltages, an average value which can be later corrected considering the usually omitted voltage drops. The proposed method applies a simple expression based on the Cauchy's formula (1841), and only the usual hypotheses of continuous current conduction mode operation and negligible voltage drops due to AC inductances and diodes are assumed. PSCAD/EMTDC time-domain simulations of P type 12- and 18-pulse ATRUs, and experimental tests with a P type 12-pulse ATRU, show the usefulness of the proposed method and validate its accuracy. Considering the results obtained in Section 5 and discussed in Section 6, it can be concluded that, when applied under supply voltage balance conditions, the new method allows results as accurate as those provided by analytical expressions available in the literature or time-domain simulations performed by any software to be obtained, making the elaboration and availability of such expressions and the performance of such simulations unnecessary. Moreover, under supply voltage unbalance conditions, this method outperforms analytical expressions available in the literature and at least equals time-domain simulations performed by any software in terms of accuracy of the obtained results, also making the elaboration and availability of more accurate analytical expressions than those available in the literature and the performance of time-domain simulations by any software unnecessary. In addition, the new method provides suitable estimates of values experimentally determined both under supply voltage balance and unbalance conditions. The applications presented in this paper show that the proposed method is an easy-to-use tool which may be extended to any other application based on multi-phase uncontrolled bridge rectifiers.

Acknowledgments

This work was supported in part by the Ministerio de Ciencia, Innovación y Universidades under Grant RTI2018-095720-B-C33, which the authors gratefully acknowledge.

Declarations

Funding: This work was supported in part by the Ministerio de Ciencia, Innovación y Universidades under Grant RTI2018-095720-B-C33.

Conflicts of interest: The authors have no conflicts of interest to declare that are relevant to the content of this paper.

Availability of data and material: Not applicable.

Code availability: Not applicable.

Authors' contributions: All authors contributed to the conception and elaboration of the present work. Material preparation, data collection and analysis were performed by Jaume Saura and Juan Jose Mesas. The first draft of the manuscript was written by Luis Sainz and all authors commented on previous versions of the manuscript. All authors read and approved the final manuscript.

References

1. Singh B, Gairola S, Singh BN et al (2008) Multipulse AC–DC converters for improving power quality: a review. IEEE Trans. on Power Electronics 23(1):260–281
2. Jiang L, Chen Q, Mao L et al (2012) Asymmetrical operation analysis of multi-pulse ATRU. In: Proc. of the 7th IEEE International Power Electronics and Motion Control Conference - ECCE Asia (IPEMC - ECCE Asia), pp. 660–665
3. Yang T, Bozhko S, Wheeler P et al (2018) Generic functional modelling of multi-pulse auto-transformer rectifier units for more-electric aircraft applications. Chinese Journal of Aeronautics 31(5):883–891
4. Yang T, Bozhko S, Asher G (2015) Functional modeling of symmetrical multipulse autotransformer rectifier units for aerospace applications. IEEE Trans. on Power Electronics 30(9):4704–4713
5. Yang T, Bozhko S (2015) Functional modelling of multi-pulse asymmetric auto-transformer rectifier units. In: Proc. of the 3rd IEEE International Conference on Electrical Systems for Aircraft, Railway, Ship Propulsion and Road Vehicles (ESARS), pp. 1–8
6. Uan-Zo-li A, Burgos RP, Lacaux F et al (2005) Analysis of new step-up and step-down direct symmetric 18-pulse topologies for aircraft autotransformer-rectifier units. In: Proc. of the 36th IEEE Power Electronics Specialists Conference (PESC), pp. 1142–1148

7. Burgos RP, Uan-Zo-li A, Lacaux F et al (2005) Analysis of new step-up and step-down 18-pulse direct asymmetric autotransformer-rectifiers. In: Conference Record of the IEEE Industry Applications Conference Fortieth IAS Annual Meeting (IAS), pp. 145–152
8. Chen J, Chen J (2018) On reducing the shaft torque ripple of small-to-medium-scale wind energy conversion systems using multi-pulse autotransformer rectifier. Energies 11(2):1–17
9. Rail Transit Vehicle Interface Standards Committee of the IEEE Vehicular Technology Society (2010) IEEE Standard for Uncontrolled Traction Power Rectifiers for Substation Applications Up to 1500 V DC Nominal Output. IEEE Std 1653.2-2009
10. Jeong S-G, Choi J-Y (2002) Line current characteristics of three-phase uncontrolled rectifiers under line voltage unbalance condition. IEEE Trans. on Power Electronics 17(6):935–945
11. Pei X, Zhou W, Kang Y (2015) Analysis and calculation of DC-link current and voltage ripples for three-phase inverter with unbalanced load. IEEE Trans. on Power Electronics 30(10):5401–5412
12. Wisutmetheekorn P, Chunkag V (2012) Digital control of an AC/DC converter using the power balance control technique with average output voltage measurement. Journal of Power Electronics 12(1):88–97
13. Rahnama M, Vahedi A, Alikhani AM et al (2018) A novel diode open circuit fault detection in three phase rectifier based on k-means method. In: Proc. of the IEEE International Conference on Industrial Technology (ICIT), pp. 600–605
14. Rahiminejad M, Diduch C, Stevenson M et al (2012) Open-circuit fault diagnosis in 3-phase uncontrolled rectifiers. In: Proc. of the 3rd IEEE International Symposium on Power Electronics for Distributed Generation Systems (PEDG), pp. 254–259
15. Lee J-U, Baek S-W, Cho K-Y et al (2017) Fault detection of three phase diode rectifier based on harmonic ratio of DC-link voltage ripples. In: Proc. of the 12th IEEE International Conference on Power Electronics and Drive Systems (PEDS), pp. 386–391
16. Sabir R, Rosato D, Hartmann S et al (2019) Detection and localization of electrical faults in a three phase synchronous generator with rectifier. In: Proc. of the International Conference on Electrical Drives & Power Electronics (EDPE), pp. 18–23
17. Kamel T, Biletskiy Y, Chang L (2015) Fault diagnoses for industrial grid-connected converters in the power distribution systems. IEEE Trans. on Industrial Electronics 62(10):6496–6507
18. Kamel T, Biletskiy Y, Chang L (2016) Real-time diagnosis for open-circuited and unbalance faults in electronic converters connected to residential wind systems. IEEE Trans. on Industrial Electronics 63(3):1781–1792
19. Saura J, Bakkar M, Bogarra S (2020) Open-circuit fault diagnosis and maintenance in multi-pulse parallel and series TRU topologies. IEEE Trans. on Power Electronics 35(10):10906–10916
20. Schade OH (1943) Analysis of rectifier operation. IEEE Proceedings of the Institute of Radio Engineers 31(7):341–361
21. Bogle AG (1977) Rectifier circuit performance: some new approximate formulas. IET Proceedings of the Institution of Electrical Engineers 124(12):1127–1134
22. Hall KS (1980) Calculation of rectifier-circuit performance. IET Proceedings of the Institution of Electrical Engineers 127 Pt. A (1):54–60
23. Hafez AAA, Yousef AM (2017) Multi-pulse diode rectifier for more-electric aircraft applications: parallel versus series topologies. Iraq J. Electrical and Electronic Engineering 13(1):138–144
24. Hykšová M, Kalousová A, Saxl I (2012) Early history of geometric probability and stereology. Image Analysis and Stereology 31(1):1–16
25. Cauchy A-L (1841) Note sur divers théorèmes relatifs à la rectification des courbes, et à la quadrature des surfaces. C. R. Acad. Sci. Paris 13:1060–1065
26. Bird BM, King KG, Pedder DAG (1993) An Introduction to Power Electronics, 2nd edn. Wiley, New York
27. Chen Q, Mao L, Ren X et al (2012) Research of the current-injection-based P-type 12-pulse ATRU. In: Proc. of the 7th IEEE International Power Electronics and Motion Control Conference - ECCE Asia (IPEMC - ECCE Asia), pp. 41–46